JOURNAL OF MATERIALS SCIENCE **39** (2004) 1759– 1763

Aging behavior and precipitation kinetics of SiCp/6061Al composites

ZHAO MIN*, WU GAOHUI, JIANG LONGTAO
School of Materials Science and Engineering, Harbin Institute of Technology, Harbin 150001, People's Republic of China
E-mail: zhaomin1920@yahoo.com.cn

The aging behavior of SiC particle reinforced 6061 aluminum matrix composites was investigated with Brinell hardness measurement, differential scanning calorimetry (DSC), scanning electron microscopy (SEM) and transmission electron microscopy (TEM). For 40 vol%SiCp/6061Al composite, the age-hardening efficiency was lower than that of monolithic 6061Al alloy and its high strength was mainly attributed to the introduction of high volume fraction particles. At low aging temperature, the aging process of composite was more accelerated than that of 6061Al alloy. With temperature increasing, the time to reach the peak hardness was shortened and the precipitation processes became accelerated. Moreover, precipitation process observed in the matrix alloy was altered by the addition of SiC particles. Formation of G.P. region was severely suppressed and the activation energy of β' phase decreased, which made the precipitation of β' phase easier than that of 6061Al alloy.

1. Introduction

Metal matrix composites reinforced with high volume fraction particles are attractive for applications requiring higher elastic modulus and strength [1]. For aluminum matrix composites, aging treatment has been widely used as an effective method to obtain stabilized microstructure and ultimate application properties [2, 3]. Extensive researches have been investigated on the aging behavior of aluminum matrix composites. These researches [4–9] indicated that aging kinetics and aging hardening efficiency of composites depended on variety of factors, such as the size, shape and volume fraction of reinforcement, fabrication method of the composites, aging temperature and so on. However, aging characteristics of high volume fraction ($\geq$30 vol%) particle reinforced composite have so far received little attention. Suresh *et al*. [10] found that with particle volume fraction increasing, there was no obvious improvement on the aging process of SiCp/Al composite. However Jun-Shanlin *et al*. [11] believed that in SiCp/Al composites the volume fraction was higher, the time to achieve peak-aged hardness was shorter, and addition of 20 vol%SiC particles accelerated the progress of aging.

The present work is aimed to investigate the effect of high volume fraction SiC particle on aging behavior and precipitation kinetics of squeeze cast 40 vol%SiCp/Al composite. The aging behavior has been examined using Brinell hardness and differential scanning calorimetry (DSC) analysis, combined with microstructure observation by scanning electron microscope (SEM) and transmission electron microscopy (TEM).

2. Materials and methods

SiC particles (40 vol%, 3.5 μm mean size) reinforced Al composites were fabricated by squeeze casting technology [12]. The aluminum matrix alloy was an Al-Mg-Si alloy (6061Al) whose nominal compositions were listed in Table I.

The composite was solution treated at 530°C for 1 h and water quenched at room temperature. After solution treatment, the alloy and composite were aged at 130, 160 and 190°C for periods up to 100 h. For comparison, the unreinforced matrix alloy was also treated as abovementioned craft.

An S-570 scanning electron microscope (SEM) was used to examine the microstructure of the composite. Brinell hardness (HB) tests were performed immediately after aging on an HBV-30 double-purpose tester with a 1 mm diameter ball indenter. A load of 30 Kgf was applied and maintained for 20 s. Each hardness value was the average of at least five measurements. Fig. 1 shows the shape and dimensions of specimen used in hardness testing as well as the indented positions.

DSC experiments were conducted immediately after solutionized and quenching treatment condition using PERKIN-ELMER thermal analyzer. The weight of sample was less than 50 mg. All DSC tests started at room temperature and terminated at 400°C, and a range of heating rates from 5°C/min to 20°C/min were used.

Transmission electron microscope (TEM) foils were prepared by a standard combination of mechanical and ion-beam thinning using a Gattan-600 ion mill equipped with liquid-nitrogen cold stage to prevent

*Author to whom all correspondence should be addressed.

TABLE I Chemical compositions of aluminum matrix alloy of composite (wt%)

Alloy	Cu	Mg	Mn	Fe	Si	Zn	Ti	Ni	Al
6061Al	0.43	0.75	0.22	0.36	1.26	<0.15	<0.05	<0.05	Bal

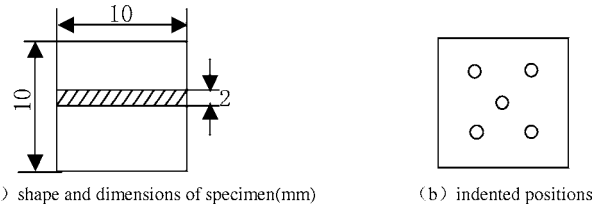

（a）shape and dimensions of specimen(mm)　　（b）indented positions

Figure 1 Shape and dimensions of hardness testing specimen and the indented positions of hardness testing.

heating during the ion-milling process. A Philips T20 electron microscope was used to characterize the microstructures at an accelerating voltage of 200 kv.

3. Results and discussion

3.1. Microstructure observation

Fig. 2 shows SEM microstructure of as-fabricated SiCp/6061Al composite used in this paper. It was found that SiC particles distributed uniformly in matrix alloy. Moreover, the composite was dense and macroscopically homogeneous, free from common cast defects such as porosity and shrinking cavities.

3.2. Aging behavior

The effect of aging time on the hardness of the SiCp/6061Al composite and the unreinforced 6061Al alloy aged at 130°C is shown in Fig. 3. Due to the addition of SiC particulates, the hardness of composites was obviously higher than that of matrix alloy. The hardness difference between composites and alloy was larger prior to the peak hardness, beyond this peak, the differences in hardness gradually became steady. The composite reached peak hardness in 9 h ,while the matrix alloy required 53 h, indicating accelerated age-

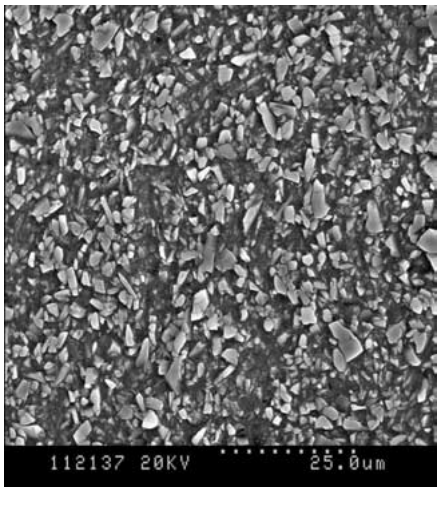

Figure 2 SEM micrograph of 40% SiCp/Al composites.

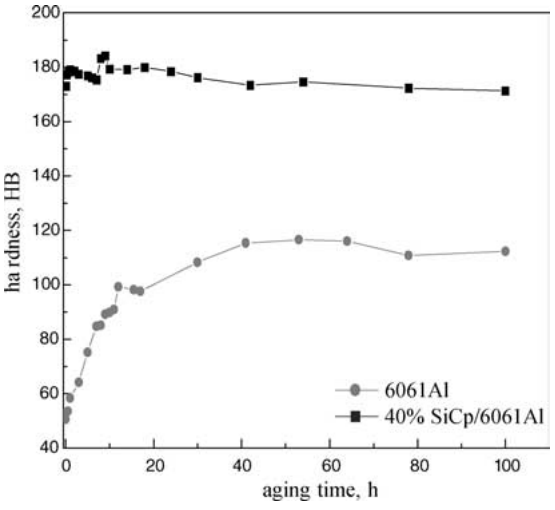

Figure 3 Aging curves for 6061Al alloy and SiCp/6061Al composite aged at 130°C.

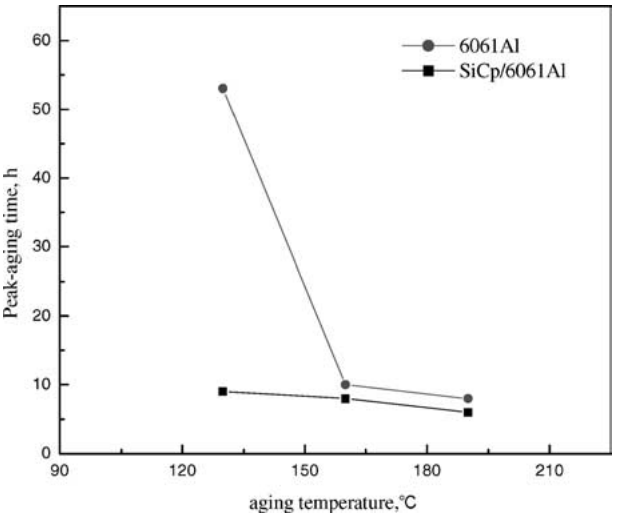

Figure 4 Effect of aging temperature on the peak-aging time for 6061Al alloy and SiCp/Al composite.

hardening in the SiCp/Al composite compared with the unreinforced 6061Al alloy at 130°C.

Fig. 4 gives the effect of aging temperature on the peak-aging time for the composite as well as unreinforced alloy. The peak-aging time decreased with increasing of aging temperature for both the alloy and composite, and the age-hardening kinetics became faster as the aging temperature increased. Under experimental temperatures, the time to achieve peak hardness was less in the composite as compared with the monolithic alloy. When the aging temperature higher than 130°C, the peak-aging time difference between the alloy and composite was very little. However, previous research [13] referred that for SiCp/Al composites at low temperature aging kinetics was more delayed than that of matrix alloy or not affected by reinforcement, which was contradicted with our results.

The effect of aging temperature on the peak hardness increment (ΔHB) for the composite as well as unreinforced alloy is shown in Fig. 5. For unreinforced matrix alloy, the hardness difference between homonization condition and peak condition was more than 60 HB. However, in case of the composite, the hardness

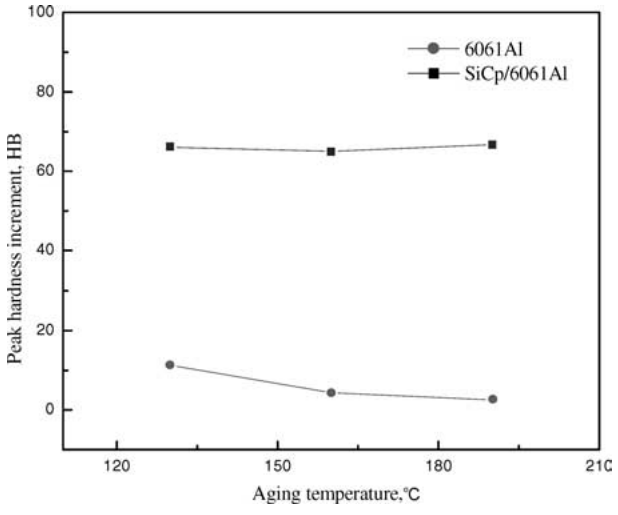

Figure 5 Effect of aging temperature on the peak hardness increment for 6061Al alloy and SiCp/6061Al composite.

difference between two conditions was less than 10 HB, which was lower than that of matrix alloy. The peak hardness increment was lower at all temperatures for the composite as compared with that of the matrix alloy, that was, the age-hardening efficiency of SiCp/Al composite was lower than that of monolithic 6061Al alloy. This may be attributed to the existence of the high volume fraction particles, which influences or alters the volume fraction or shape of precipitates in matrix alloy to affect aging behaviors of composite. And the further discussion is in what follows. Hunt *et al*. [14] showed that the hardness enhancement of SiCp/Al composites after natural aging was lower than that of matrix alloy. But in this paper, for high volume fraction composite, after artificial aging, the degree of hardness improvement was lower than that of matrix alloy.

Therefore, for high volume fraction SiCp/Al composite, the age-hardening efficiency was lower than that of monolithic 6061Al alloy. High strength was mainly attributed to the introduction of high volume fractions particles, which makes the time to peak hardness less and comparatively at low aging temperature the aging process advanced more than that of the monolithic alloy.

3.3. DSC analysis

Fig. 6 shows the DSC thermograms of the composite and matrix alloy. There were three exothermic peaks in Fig. 6a, but there was only one exothermic peak in the range of 50–400°C in Fig. 6b. Generally, peak corresponding to G.P. zone formation and dissolution should be present on the lower temperature parts of DSC plots, while no obvious peak associated with G.P. zones was observed under four different heating rates in Fig. 6b. According to previous research on the aging behavior of 6061Al alloy [15–17], three exothermic peaks in Fig. 6a respectively corresponded to the formation of G.P. (I) zones (A), G.P. (II) zones (B) and β' phase (C), one exothermic peak in Fig. 6b corresponded to the formation of β' phase. Moreover, exothermic peak corresponding to β' phase in alloy was very sharp, but that in composite was rather gentle, which revealed that precipitation temperature range of β' phase in composite was wider than that in matrix alloy.

Therefore, it can be seen that the age-hardening process and aging precipitation products in the composite were different from those in the 6061Al alloy, and the formation of G.P. zone was seriously suppressed. This may be attributed to the following possible reasons. First, the formation of G.P. was inherently slow. And higher density dislocations were induced in the composite due to the large differences in the coefficient of thermal expansion between the SiC particles and the 6061Al alloy, which offset some vacancies and made vacancies obviously sunk to reduce. In addition, high volume fraction particles themselves also limited the aggregation of vacancies. Therefore, precipitation of G.P. zone, which was mainly dependent on the gathering of vacancies, was seriously suppressed. Secondly, at the same time the addition of high volume fraction particles also pulled in a lot of interfaces, which can trap vacancies to reduce the whole concentration of vacancies in matrix alloy. The decrease in vacancies concentration had a strong influence on the nucleation of G.P. zone. So the formation of G.P. was depressed far away. Even no obvious G.P. peak in DSC curves was found, which was different from that of unreinforced matrix alloy (seen in Fig. 6).

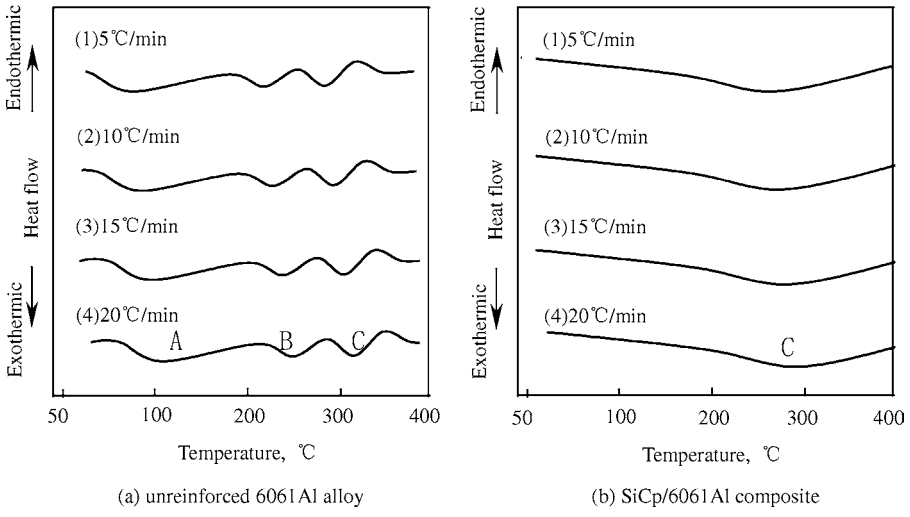

Figure 6 DSC thermograms for the as-quenched 6061Al alloy and SiCp/Al composites at different heating rates.

TABLE II Temperature of exothermic peak of SiCp/6061Al composites and 6061Al alloy

Materials	Heating rates (°C/min)	Peak temperatures (°C) G.P. (I)	G.P. (II)	β'
6061Al	5	81.4	236.6	280.7
	10	87.0	243.6	287.4
	15	93.7	252.3	302.0
	20	103.7	262.6	315.6
SiCp/6061Al	5	–	–	259.3
($V_f = 40\%$)	10	–	–	268.7
	15	–	–	278.6
	20	–	–	290.5

Furthermore, Table II shows temperature of exothermic peak for SiCp/6061Al composite and 6061Al alloy. It followed that exothermic peaks were shifted to higher temperature with increasing of heating rate. At all heating rates, the peak temperature of β' phase precipitation in the composite was lower than that in the monolithic alloy, which revealed that the precipitation kinetics was accelerated by the addition of SiC particles.

3.4. Calculation of thermal diffusion activation energy

Thermal diffusion activation energy during precipitation process can be calculated according to the following equation of Augis and Bennett [18]:

$$\ln[(T_p - T_0)/Q] = -\ln K_0 + E/RT_p \qquad (1)$$

where T_p represents exothermic peak temperature of precipitates, T_0 represents initial temperature, Q represents the heating rate, K_0 represents reactive constant, E represents thermal diffusion activation energy and R represents gas constant 8.314 J/mol.

Results shown in Table II was put in formula (1) to make a graph of a relationship between $\ln[(T_p - T_0)/Q]$ and $1/T_p$, then points determined by four heating rates were made to fit a straight line, and the slope coefficient of that line was $\tan\theta$:

$$\tan\theta = E/R \qquad (2)$$

According to formula (2), thermal diffusion activation energy of different precipitates in two materials can be calculated, as shown in Fig. 7. It can be clearly seen that thermal diffusion activation energy of β' phase in composite was 98.64 KJ/mol, while in matrix alloy it was up to 144.93 KJ/mol. Obviously, thermal diffusion activation energy in composite was lower than that in matrix alloy, which indicated that lower energy was needed to form β' phase in composite. That is to say, the precipitation of β' phase was accelerated. This calculation results were coinciding with the observation results in Table II.

It followed that introduction of high volume fraction particles made the precipitation in composite different from that in unreinforced matrix alloy, which was verified by DSC testing. The addition of high

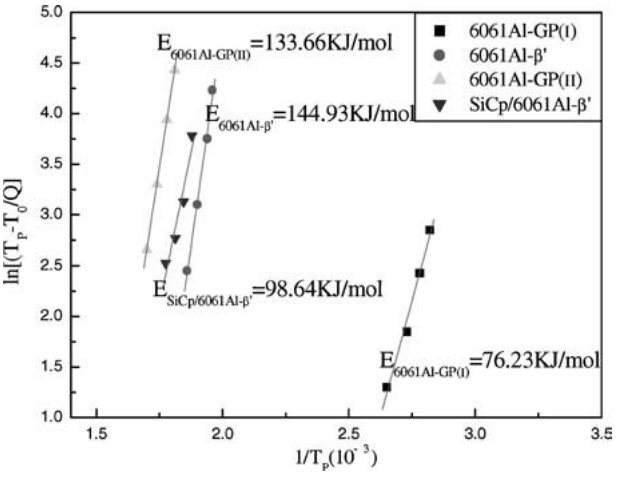

Figure 7 Comparison of thermal diffusion activation energies of various precipitates.

volume fraction SiC particles significantly accelerated age kinetics of the aluminum matrix alloy, which was consistent with most researchers' conclusions [7–9]. However, the formation of G.P. region was severely suppressed and the activation energy of β' phase was decreased, which made the precipitation of β' phase easier than that of 6061Al alloy.

3.5. TEM observation

The TEM morphology of SiCp/6061Al composites aged at 160°C for 40 h is shown in Fig. 8. Rod like β' precipitates was observed and precipitation of β' phase were coarse under over-aged condition. In addition, the precipitates were inclined to each other at an angle and two mutually perpendicular directions for the precipitates dominated the microstructures. And β'precipitates in matrix alloy which have formed heterogeneously on dislocations, were consistent with the observations of Dutta *et al*. [16]. Under over-aged condition, most of dislocations were exhausted, while discontinuous precipitates at the dislocations can also be observed in composite matrix (as pointed in Fig. 8). The characteristic ⟨110⟩ of the matrix 6061Al alloy is quite apparent in the diffraction patterns shown along with the micrographs in Fig. 8b. In general, though the precipitation of G.P. zones in composite was suppressed, the residual stresses and high density dislocations (seen in Fig. 9) as well as interfaces introduced by the presence of high volume fraction SiC particles provided favorable locations for non-uniform nucleation of β' phase, which reduced the nucleation incubation period and accelerated nucleation precipitation. On the other hand, high density dislocation made Mg and Si *et al*. atoms diffuse faster, which reduced the formation energy of β' phase and promoted β' phase precipitation. That was corresponding with the results of DSC analysis. Furthermore, in this composite, the volume fraction of the particles was 40%, namely there was only 60 vol% matrix alloy. Although the aging process was accelerated and the thermal diffusion activation energy of β' phase was reduced, in general, the magnitude of precipitates was less than that of the unreinforced matrix alloy. So

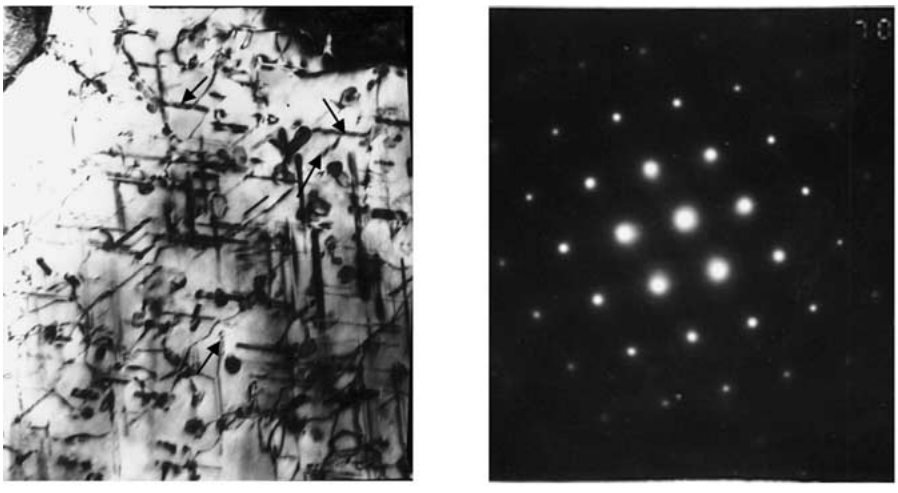

(a) morphology (b) 〈110〉 SADP from the matrix of 6061Al alloy

Figure 8 TEM micrographs of SiCp/Al composite aged at 160°C for 40 h.

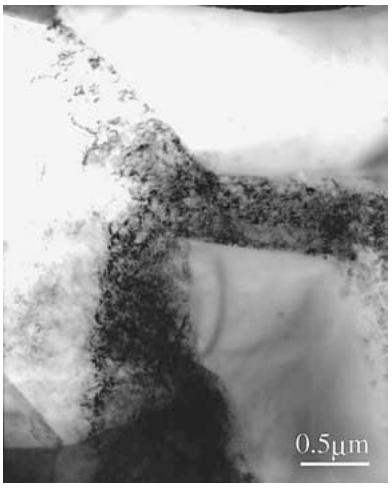

Figure 9 High-density dislocations in the composite.

the age-hardening efficiency of SiCp/Al composite was lower than that of the monolithic 6061 alloy.

4. Conclusions

1. Introduction of high volume fraction particles, which brought high-density dislocations and interfaces *et al*., made the precipitation of the composite different from that of unreinforced matrix alloy. The age-hardening efficiency of SiCp/Al composite was lower than that of the monolithic 6061 alloy. High strength was mainly attributed to the introduction of high volume fractions particles.

2. Aging temperature had great effect on the hardening process. Comparatively, at low aging temperature aging process was more accelerated than that of 6061Al alloy. With the increasing of temperature, the precipitation process became accelerated, and the time to reach peak hardness was shortened.

3. Addition of high volume fraction SiC particles significantly accelerated age-hardening kinetics of the aluminum matrix alloy. The formation of G.P. region was severely suppressed and the activation energy of β' phase decreased due to the addition of SiC particles, which causes the precipitation of β' phase easier than that of 6061Al alloy.

Acknowledgements

This research is supported by National Natural Science Foundation of China under Grant No. 59771014 and No. 50071019. The supports are gratefully acknowledged.

References

1. S. W. LAI and D. D. CHUNG, *J. Mater. Sci*. **24** (1994) 6181.
2. I. J. POLMEAR and S. P. RINGER, *J. JILM* **50** (2000) 633.
3. Q. G. WANG and C. J. DAVIDSON, *J. Mater. Sci*. **36** (2001) 739.
4. D. J. TOWLE and C. M. FRIEND, *Scripta Metall. Trans.* **26** (1992) 437.
5. V. MASSARDIER, L. PELLETIER and P. MERLE, *Mater. Sci. and Engng*. A **249** (1998) 121.
6. M. GUPTA, S. QIN and L. W. CHIN, *J. Mater. Process. Techn*. **65** (1997) 245.
7. T. DAS, P. R. MUNROE and S. BANDYOPADHYAY, *J. Mater. Sci*. **31** (1996) 5351.
8. C. SHEN and S. LIN, *ibid*. **32** (1997) 1741.
9. Y. SONG and T. N. BAKER, Mater. Sci. Techn. **10** (1994) 406.
10. S. SURESH, T. CHRISTMAN and Y. SUGIMURE, *Scripta Metall*. **23** (1989) 1599.
11. J. S. LIN, P. X. LI and R. J. WU, *Scripta Metall. Mater*. **28** (1993) 281.
12. WU GAOHUI, Patent of the People's Republic of China, 94114284.X (in Chinese).
13. DONG SHANGLI and YANG DEZHUANG, *J. Mater. Eng*. **8** (1996) 38 (in Chinese).
14. E. HUNT, P. D. PITCHER and P. J. GREGSON, *Scripta Metall. Mater* **24** (1990) 937.
15. MA WENCHUAN and GU JIALIN, *J. Mater. Sci. Lett*. **16** (1997) 1867.
16. I. DUTTA, S. M. ALLEN and J. L. HAFLEY, *Metall. Trans.* **22A** (1991) 2553.
17. HIROYUKI TODA, TOSHIRO KOBAYASHI and MITSUO NIINOMI, *J. Japan Inst. Metals* **56** (11) (1992) 1303.
18. J. A. AUGIS and J. E. BENNETT, *J. Thermal Anal*. **13** (1978) 283.

Received 10 October 2002
and accepted 6 November 2003